Interference Modelling and Analysis of Random FDMA schemes in Ultra Narrowband Networks

Minh-Tien Do

Sigfox Wireless Company
Labège, France
Email: minhtien.do@sigfox.com

Claire Goursaud and Jean-Marie Gorce

INSA-Lyon, CITI-Lab
Lyon, France
Email: claire.goursaud@insa-lyon.fr
jean-marie.gorce@insa-lyon.fr

***Abstract*—Ultra narrow band (UNB) transmission is a very promising technology for low-throughput wireless sensor networks. This technology has already been deployed and has proved to be ultra-efficient for point-to-point communications in terms of power-efficiency, and coverage area. This paper introduces this technology and gives some insights on the scalability of UNB for a multi-point to point network. In particular, we present a new multiple access scheme: random frequency division multiple access (R-FDMA) and study the impact of the induced interference on the system performance in terms of bit error rate and outage probability. To this aim, we propose and design a simplified model to describe the interference impact. Thanks to this model, we theoretically derive BER and OP expressions for the lower, approximated and upper case. This enables us to evaluate the performance capacity, by determining the maximum number of simultaneous users that can be served.**

***Keywords*–Wireless sensors networks; M2M/IoT applications; Random FDMA; Aggregate interference; Ultra narrow band.**

I. INTRODUCTION

In current trend, the internet of things (IoTs) and wireless sensor networks (WSNs) share many common constraints [1], and thus, the communication techniques applied for WSNs could be reused for IoTs and machine-to-machine (M2M). The challenges are the connection of countless wireless devices and the requirement of cost-effective, power-efficient and scalable network. In networks for applications, such as temperature monitoring, electrical metering etc., nodes send dynamically a small amount of data. As a consequence, a high bit rate is not mandatory for each link. Therefore, ultra narrow-band (UNB) transmissions can be used for such low-throughput networks.

UNB consists of sending the information occupying a very narrow frequency band with the binary-phase-shift-keying (BPSK) modulation. The BPSK modulation is used because it satisfies power-efficiency, bandwidth-efficiency and cost-effectiveness for low-throughput network in long range communication [2]. Besides, as the occupied band is reduced, the noise contribution is lessen at the receiver. Consequently, for a given targeted error probability, the reception power sensitivity is very low, enabling a very large coverage area using a single base-station (more than 50 km in open field).

With such an extended coverage, a large amount of source nodes are eligible to be served and will compete for transmission. Thus, the medium access control (MAC) protocol is important to consider. The contention-free channel access methods are not efficient with respect to the low quantity of information to be transferred and would lead to a waste of time for protocols or synchronization issues. Contrarily, the random access protocols are a promising solution, as they present more flexibility to manage bursty and random transmissions.

As verified in [3][4], most of the MAC studies consider that the nodes share the same frequency channel, and focus on the decision of the moment to transmit. Nonetheless, studies on the multi-channel MAC also consider the frequency as a random variable [5][6][7]. However, these studies consider predefined disjoint channels, which is not a realistic assumption in UNB networks. Indeed, at typical transmission frequency 800 MHz, and a typical oscillation jitter 0.5 ppm - 2 ppm, there is an uncertainty on the frequency positioning is around 400 Hz, which is bigger than the transmission band. As a consequence, with UNB technology, random frequency multiple access (R-FDMA) scheme has to be considered, as we proved in [8]. The network behaves as if each node transmitted in a bursty way to access to the medium, and at a frequency chosen randomly in the available bandwidth.

Consequently, at the PHY layer, besides the effect of classical channel impairments such as fading, shadowing effect, inter-symbol interference and noise [9][10], in R-FDMA scheme, the system performance depends also on the carrier frequency distribution and the corresponding interference term resulting from physical channels overlap. While the performance of the single link is easy to obtain, no accurate model for multiple links has been proposed. Specifically, the behavior of the interference induced by a large number of unconstrained nodes (both in time and frequency) over a wide area around the sink has not yet been studied. For certain classes of node distribution, most notably Poisson point processes, and attenuation laws, closed-form results are available for both interference term and signal-to-interference ratios (SIR), which determine the network performance [11][12][13][14][15]. However, as in MAC studies, the users are either transmitting in the same channel (i.e., with the same carrier frequency: thus highly interfering), or in adjacent channels (thus barely interfering). But, in the case of continuous R-FDMA, the frequencies are selected in a continuous way in the total band and lead potentially to all values, independently of the path-loss. Therefore, a new analysis of the system performance needs to be done, to take into account this new specificity.

In this paper, we propose to study the interference of Random FDMA schemes in UNB network. We characterize the system performance by understanding and modeling the distribution of the aggregate interference power (AIP). The others channel impairments are neglected. We propose an approximation for the AIP and derive a closed-form of the probability density function (PDF) of channel interference. This enables us to provide an upper and lower bound beyond to estimate the system performance.

The rest of the paper is organized as follows. Section II presents the wireless network model for UNB and describes the considered R-FDMA scheme. In Section III, we present the theoretical interference analysis and simplified models that are used in next section for the system performance evaluation. Then, the estimated capacity network using the simplified models are presented in Section IV. Finally, we conclude in Section V.

II. Transmission Model

A. Ultra Narrow Band Transmission

UNB refers to the fact that the individual bands used at the transmission sides are very narrow compared to the whole available bandwidth (typically 1:100). While digital or analog data of narrow band radio system are transmitted and received over a few kHz [9], UNB signals require around 100 Hz only, which can be achieved with highly selective FIR filters. Such transmissions have several benefits: flat fading can be assumed, which highly simplifies the system analysis and the receiver, while a higher number of users can be supported.

UNB technology is currently deployed, e.g., in Sigfox's networks [16]. In these deployments, a star topology is used, where base-stations centered in large cells receive the data from a huge amount of source nodes spread over. Because of the ultra narrow spectral occupation, the noise contribution is very low (around -150 dBm at $T = 290$ K). So, contrary to classical deployments, such technology enables an exceptionally large-scale wireless connection thanks to the ability to successfully demodulate an extremely low received power signal (-142 dBm). These advantages allow data transmission in highly constrained environments where former technologies cannot operate and a possibility to cover a very large area with a very small number of base stations, reducing network management and deployment fees of several orders of magnitude.

B. R-FDMA Scheme Definition

In a random access frequency network, four main problems must be considered: the asynchronicity access of node in the wireless medium, randomness both in time and frequency domain and lack of contention based protocols. To illustrate the system behavior, a toy-example is schematized in Fig.1. It represents the time and frequency use of the channel for 4 active users.

The *randomness in time domain* has an impact on the number of users N that will be active at the same time. This value depends on several parameters: the number of possible users in the cell, the length (in time) of the packet to transmit, and the periodicity of the transmission. We present our results as a function of $k = N - 1$ the number of interfering users.

Furthermore, the *asynchronicity* permits to suppress the traffic overload needed for synchronization, but leads to varying interference levels during the transmission of a given packet, as packets do not start (and stop) at the same time. In order to simplify the analysis discussed in this work, we will not evaluate the performance evolution during the whole packet transmission, but only at a given point in time. For example, in Fig.1, at $t = t_0$ only 3 users among the 4 users are transmitting.

The *randomness in frequency domain* has an impact on the position of each active users carrier in the total band. Thus, it affects the interference suffered by a given user, which depends on the spacing δ_f between the users carrier frequency and the interferers one. The Random FDMA schemes could be divided into two kinds of frequency randomness [8] continuous and

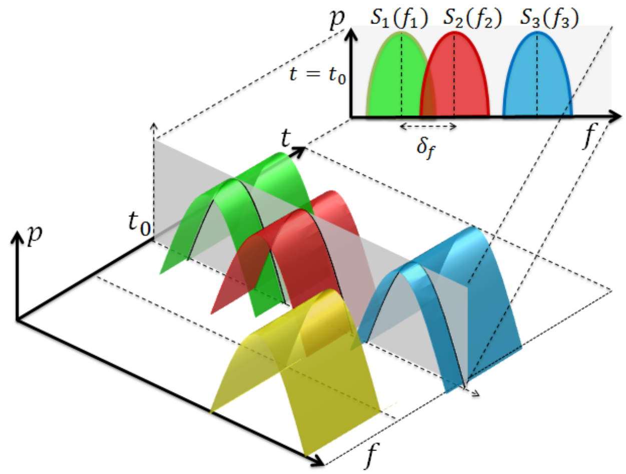

Figure 1: Example of temporal & spectral repartition of users.

discrete. In the discrete case, the carriers are chosen at random in a discrete and pre-defined subset of frequencies. But, in order to take into account the carrier imprecision due to the jitter, we consider only continuous random frequency division multiple access, where the carriers can be chosen at random in the continuous available frequency band. In this case, from the receiver point of view (i.e., on base-station side), the monitored bandwidth is filled from time to time with a set of signals of interest occupying a small amount of total spectrum and centered around unpredictable carrier frequencies. Thus, in order to handle demodulation, efficient software defined radio algorithms have been designed to analyze the total band, determine transmitter activity and retrieve data they are transmitting. These algorithms are currently deployed in SigFoxs network, and do not fall in the scope of this paper.

The *lack of contention based protocols* implies that each user is transmitting without any knowledge of carrier frequencies being used in the cell. Thus, this induces interference (when at least 2 users are transmitting at the same moment and there is an overlap between the individual transmission bands). For example, in Fig.1, the green user starts transmitting even if the red one is already using the band in common.

Furthermore, we should note that R-FDMA allows the use of transmitters whose frequency is unconstrained (except for being in the transmission bandwidth). In practice, the randomness in frequency domain is easily done: each node has its own transmission frequency, which it not controlled by the network, but defined by the node components (electrical components an oscillator jitter), and may vary naturally (depending on different parameters such as temperature and age of the device). Thus, factory constraints are relaxed, and the network will not be sensible to temperature variations and other environmental parameters that can affect the carrier. Thus, cheaper nodes can be used.

As a consequence, R-FDMA is promising for smart metering where a massive amount of devices have to be connected to the Internet, provided that the randomness does not highly degrade the performances.

C. System Mathematical Model And Parameters

As described in the previous section, the main characteristic of the considered network using R-FDMA at a given point of time is that each active user is transmitting at a carrier

Copyright (c) IARIA, 2014.ISBN: 978-1-61208-360-5

frequency randomly chosen in a given band. As a consequence, interference contribution is non-controlled and can lead to transmission errors. Consider a multiple access channel with $N = k + 1$ active transmitters (note that N is much smaller than the number of nodes that are actually in the cell). The total received signal at the base-station can be expressed as:

$$r(t) = \sum_{i=1}^{k+1} s_i(t) \cdot g(f_i, t) \otimes h_i(t) + n(t) \tag{1}$$

where $s_i(t), \forall i \in [1, \ldots, k+1]$ are the BPSK symbols sent by the active user i, $g(f_i, t)$ the impulse response of the emission FIR filter (centered at f_i); $h_i(t)$ is the path-loss of the corresponding link, and $n(t)$ is an additive white Gaussian noise with zero mean, and whose variance is σ^2.

For the sake of simplicity in this analysis, we consider that $h_i(t) = \delta(t)$, $\forall i \in [1, \ldots, k+1]$. This corresponds to the worst case where all users are at the same distance of the base station and experience the same flat channel. At the base station, the received signal is analyzed to track possible transmissions in the total band (BW), and filtered at the desired frequency. Without loss of generality, we consider in this paper that the desired user is #1. The signal used for data recovery is thus:

$$r^{'}(t) = r(t) \otimes g(f_1, t) \tag{2}$$

$$= \sum_{i=1}^{k+1} s_i(t) \cdot g(f_i, t) \otimes g(f_1, t) + n(t) \otimes g(f_1, t) \tag{3}$$

To evaluate the system performances, we use the signal to interference plus noise ratio (SINR), which is expressed as:

$$\text{SINR} = \frac{P_s}{N_{tot} + P_I} \tag{4}$$

where P_s is the received power of the desired user, P_I the aggregate interference, and N_{tot} the noise contribution. These powers are estimated at a given time, and normalized with respect to $P_s = |G(f_1, t)|^2$ with $G(f_1, t)$ the frequency response of the FIR filter. The value of P_I depends on the spacing between the carriers frequency, and its estimation will be described in the next section. We deduce the bit error rate (BER) of the BPSK transmission from the SINR as follow:

$$\text{BER(SINR)} = Q(\sqrt{SINR}) \tag{5}$$

A data transmission is considered successful if the received BER is below a predefined threshold $\beta = 10^{-3}$, otherwise, the data are considered lost. Thus, we consider the outage probability (OP) being expressed:

$$Pr(OP) = Pr(BER \geq \beta) = Pr(BER \geq 10^{-3}) \tag{6}$$

The simulation results shown in Section III and IV, the BER and OP are obtained with respect to (5), (6) (with a noise power 100 dB under the signal of interest).

III. Theoretical Interference Analysis

As described in Section II, the R-FDMA scheme solves a waste of communication resources for WSNs where the users send a short message. However, it leads to interference that must be quantified. Therefore, the goal of this study is to analyze the aggregated interference power (AIP) and propose the simplified model for UNB network based on R-FDMA scheme.

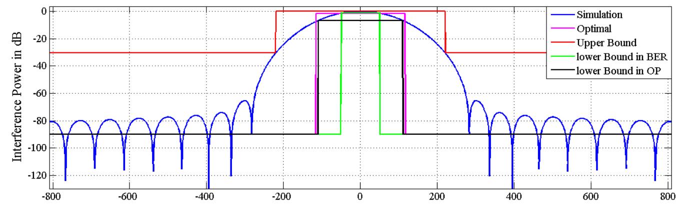

Figure 2: Behavior of interference vs frequency difference δ_f.

A. Modelization of a single interferer contribution

In the single interferer case, we consider the interference power created by a unique interferer. We assume that there are only $N = 2$ active users using R-FDMA scheme (i.e., the useful signal and $k = 1$ interfering signal). The interference power can be derived at a given time by multiplying the frequency responses of the useful signal and interfering signal.

$$P_I(t) = \mid G(f_1, t) \cdot G(f_2, t) \mid \tag{7}$$

In (7), the only parameter that will influence $P_I(t)$ is the relative frequency positioning $\delta_f = |f_1 - f_2|$ between the carriers used by the active users. Therefore, we model the interference level as a function of the frequency shift between the 2 active users $\delta_f = |f_1 - f_2|$:

$$P_I(t) = \mid G(f_1, t) \cdot G(f_2, t) \mid = P(\delta_f, t) \tag{8}$$

From now on, as we focus on the interference at a given sample time normalized to P_s, we neglect the time variable in the mathematical expressions. In Fig.2, we represent the interference evolution as a function of the frequency difference (8). The blue curve corresponds to the interference in a realistic case. We can observe that the interference is lowered if the frequency difference δ_f of two carriers is large enough. However, we should not neglect the interference caused for high δ_f. Indeed, in the case of a high interfering number, the interference will aggregate, and can lead to errors. On the contrary, a unique user will cause a significant amount of interference only if δ_f is very small, as the filter is very selective. Thus, we can observe there are 2 main areas, whose transition occurs around 200 Hz, depending on the considered criterion. In the first area, i.e., for high δ_f, the interference level is low, and mainly concentrated around -90 dB. Contrarily, in the second area, i.e., for low δ_f, the interference level is more important (up to 0 dB when using the same frequency), and almost uniformly distributed. Nevertheless, the considered band is much larger than 200 Hz (at least 12 kHz), and thus, at this scale, the interference level can also be approximated by a constant.

Therefore, we model the interference by a rectangular function:

$$I(\delta_f) = \begin{cases} I_{max} & \text{for } \mid \delta_f \mid \leq \triangle/2, \\ I_{min} & \text{for } \mid \delta_f \mid > \triangle/2. \end{cases} \tag{9}$$

where $\triangle$ corresponds to the width of δ_f that creates high interference level. The first line corresponds to low δ_f interferers, and the second one to high δ_f interferers.

The simplified model can be used to define the upper and the lower bound of the interference pattern. For the upper bound, the maximum level can be easily identified in Fig.2, and is set to the maximum interference power i.e., $I_{max\ up}(\delta_f = 0) = 0$ dB. On the contrary, the minimum level

Copyright (c) IARIA, 2014.
ISBN: 978-1-61208-360-5

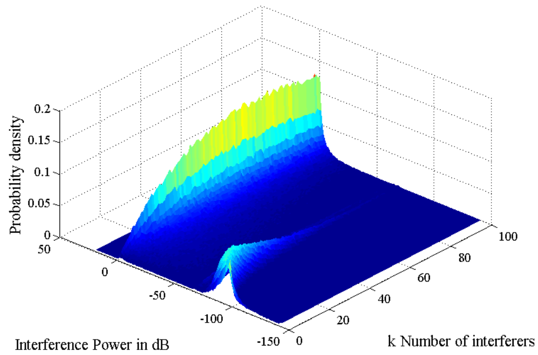

Figure 3: PDF of the aggregate interference power [dB], for $k = 100$ interferers, for BW = 12 kHz.

$I_{min\ up}$ and the width $\triangle_{up}$ can take many values, but should verify:

$$I_{min\ up} = P(\triangle_{up}) \quad (10)$$

For the lower bound, the known characteristic is the minimum level, which is set to $I_{min\ low} = -90$ dB (we neglect the lower interference values as they occur with a very low probability), whereas the other two parameters are jointly are jointly defined such as:

$$I_{max\ low} = P(\triangle_{low}) \quad (11)$$

We can also define an approximated model with unconstrained parameters $(\triangle, I_{min}, I_{max})$. We consider that $I_{min} = -90$ dB, which is the most frequent interference value, the optimal rectangular model is defined by the couple $(\triangle, I_{max})$. The bound and approximation model parameters are derived in the next section.

B. Modelization of a multi-interferers contribution

As in practice, the network will support more than 2 active users in practice, we further our study by considering more users based on R-FDMA scheme and in a realistic deployment. In this section, we aim at quantifying the cumulative interference and its influence on the system performance.

To characterize the interference statistics, we used a Monte Carlo simulation with number of repetitions: 10^4, for a network containing up to $k = 100$ interferers ($N = 101$ active nodes), deployed randomly over a continuous bandwidth of BW = 12 kHz. For the sake of simplicity, we suppose that the desired user is transmitting in the middle of the total band. Besides simplicity, this case corresponds to the worst case. Indeed, at this central frequency, the desired user will suffer from statistically more interference than any other active user. This is due to the fact that the average δ_f is smaller in this case. We have evaluated the aggregate interference power (AIP) and observe its Probability Density Function (PDF) distribution. Simulation results are presented in Fig.3.

We can verify that if the number of nodes is small, the power level of AIP remains very small and is mostly situated in the interval from -60 to -90 dB. Contrarily, when the number of node increases, the AIP gradually converges to the left, near 0 dB (which corresponds to $\delta f = 0$ for a single interferer case) and more. In fact, when the number of active users increases, the probability that at least one user chooses a frequency close to the receiver of interest is also increased. This contribution will dominate the others, and lead to a high level of interference. Finally, we can point out that the interference evolution is not trivial. Indeed, we can note 2 areas of interest (-90 dB and 0 dB) where the probability is dominant. Therefore, as shown in Fig.2 and Fig.3, the AIP cannot be approximated by a classical model, such as a Gaussian approximation for example, because, it does not take into account both main lobe for small δ_f, and side lobe for large δ_f, even for a unique interferer. But, as the interference is difficult to model exactly, we have chosen to use the rectangular model, to estimate the network AIP.

In (9), as the interference created by a unique user is supposed to take only 2 values, we distinguish 2 kinds of interferers:

– Those whose frequency shift is $| \delta_f | \leq \triangle/2$ and create interference level I_{max}. We call n_L the number of such users. The probability for an user to be in this category is $p = \frac{\triangle}{BW}$.

– The others, which create interference level I_{min}. We call $n_P = k - n_L$ the number of interferers in this case.

Thus, the total aggregate interference power I_{tot} created by k active interferes is:

$$I_{tot}(k, n_L) = n_L \cdot I_{max} + (k - n_L) \cdot I_{min} \quad (12)$$

Besides, the probability to have exactly n_L users among the k ($\forall n_L \in [0, 1, ..., k]$), that creates an interference of I_{max} is:

$$Pr(N_L = n_L) = C_k^{n_L} \cdot p^{n_L} \cdot (1 - p)^{(k - n_L)} \quad (13)$$

Thus, from (4), (5) and (6), the BER and OP can be obtained with:

$$BER(k) = \sum_{n_L=0}^{n_L=k} Pr(N_L = n_L) \cdot Q\left(\sqrt{\frac{P_s}{I_{tot}(k, n_L)}}\right) \quad (14)$$

$$OP(k) = \sum_{n_L / I_{tot}(n_L) > \beta} Pr(N_L = n_L) \quad (15)$$

The (14) and (15) can be used for whichever rectangular model, in general, for the upper and lower bound, and for the approximation in particular. By using root mean square (RMS), we have evaluated the RMS_{BER} and RMS_{OP} as a function of $\triangle$ for the lower and the upper bound. Then, we have deduced consecutively the values $I_{min\ up}$ and $I_{max\ low}$ with (10) and (11). Indeed, the results using the simplified model have been compared to simulation ones (with RMS metric performed in the logarithmic scale so as to ensure a good approximation for whichever magnitude degree) to determine the best width $\triangle$ and the corresponding interference level. This study has been done for several bandwidths (BW).

As shown in Fig.4, the minimal RMS is independent of BW. For upper bound, the optimal width is obtained for $\triangle_{up} = 440Hz$ in term of both BER and OP. On the other hand, for lower bound, the optimal width in term of BER and OP will be respectively $\triangle_{low} = 100$ Hz and $\triangle_{low} = 220$ Hz. The obtained upper and lower bounds models are represented in Figure2.

We can also use these equations to empirically evaluate $(\triangle, I_{min}, I_{max})$ that are the most accurate from (9). We have evaluated the RMS_{BER} and RMS_{OP} as a function of the couple $(\triangle, I_{max})$. We have compared (with log-scale RMS metric) the BER and OP obtained with the theoretical model, and by simulation for $BW = 12$ kHz. Results obtained with a sampling precision of 1Hz and 0,005 dB are presented in Fig.5 and Fig.6. We can observe that, the width $\triangle$ has little impact on the BER accuracy, while I_{max} has little impact on

Copyright (c) IARIA, 2014. ISBN: 978-1-61208-360-5

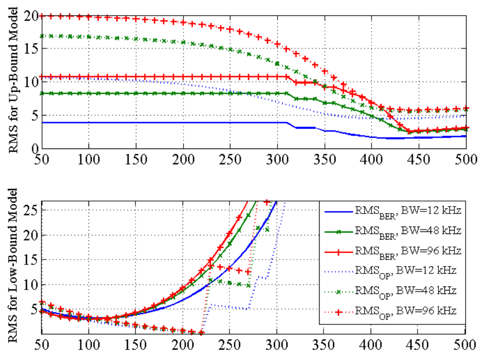

Figure 4: RMS for BER and OP vs $\triangle$, for $k = 100$, different bandwidth length.

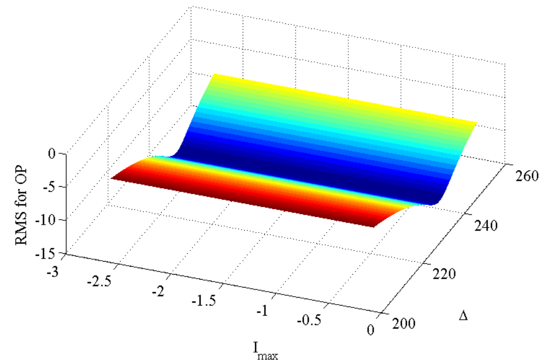

Figure 6: RMS for OP vs the couple $(\triangle, I_{max})$, for $I_{min} = -90$ dB, $k = 20$ interferers and $BW = 12$ kHz.

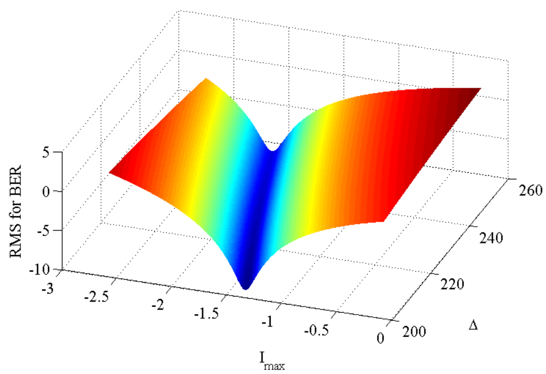

Figure 5: RMS for BER vs the couple $(\triangle, I_{max})$, for $I_{min} = -90$ dB, $k = 20$ interferers and BW=12 kHz.

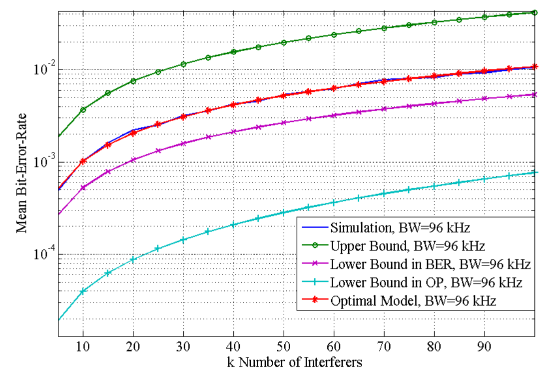

Figure 7: Mean BER as a function of k interferers, for BW = 96 kHz.

the OP accuracy. Thus, regarding the OP criterion in Fig.6, we get the best approximation for $\triangle = 232Hz$. On the contrary, in Fig.5, we identified $I_{max} = -1.77$ dB as the best one for BER. Therefore, the couple ($\triangle = 232$ Hz, $I_{max} = -1.77$ dB) is considered as the optimal one (plotted in Fig.2) for both OP and BER approximation.

We validate the accuracy of our models (lower bound, upper bound and approximation) by considering a higher bandwidth, i.e., $BW = 96$ kHz. We present in Fig.7 and Fig.8 the comparison between the average BER and OP obtained by simulation, and obtained with our theoretical models. We can first verify the accuracy of the lower and upper bounds as they provide a coherent interval for the capacity. Besides, we can note that the lower bound obtained with the BER criterion is equally pertinent for the BER and OP evaluation. On the contrary, the one obtained with the OP criterion is tight for the OP, but much too loose for the BER. Finally, we can observe that the approximation model is very accurate, even for a higher bandwidth (and thus a higher supported number of users). Thus the proposed models are consistent.

IV. Estimated Capacity Network

In this section, we estimate the system capacity in terms of the maximum number of users that can be simultaneously active; while verifying the targeted BER or OP constraint. We report in Table I, Table II and Table III, the system capacity

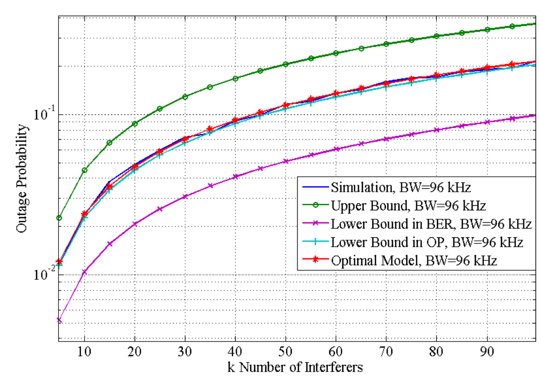

Figure 8: OP as function of k interferers, for BW = 96 kHz.

using the bounds and optimal model, and compare them with results obtained by simulation.

We can further confirm the accuracy of the bounds and optimal model. Besides, obviously, the capacity increases with the available bandwidth, and the targeted BER. However, we can note that the evolution is not linear. Indeed, e.g., when the bandwidth is increased by 8 (from 12 kHz to 96 kHz), the capacity is increased by 7.3 (from 6 to 44). Indeed, it is different to distribute N users in a B total bandwidth than

Copyright (c) IARIA, 2014. ISBN: 978-1-61208-360-5

TABLE I: Maximum Transmitters Numbers For $BER = 10^{-3}$

BW	N up	N simu	N optimal	N low (BER)	N low (OP)
12 kHz	1	2	2	3	16
24 kHz	1	3	3	5	31
48 kHz	2	5	6	10	61
64 kHz	2	7	7	13	80
96 kHz	3	10	11	20	119
1 MHz	28	103	104	199	1263

TABLE II: Maximum Transmitters Numbers For $BER = 10^{-2}$

BW	N up	N simu	N optimal	N low (BER)	N low (OP)
12 kHz	4	12	13	24	63
24 kHz	7	25	24	46	124
48 kHz	14	47	48	92	244
64 kHz	18	64	63	122	323
96 kHz	27	93	94	183	479
1 MHz	157	954	976	1918	5166

TABLE III: Maximum Transmitters Numbers For $OP = 10^{-1}$

BW	N up	N simu	N optimal	N low (BER)	N low (OP)
12 kHz	3	6	6	13	6
24 kHz	6	11	11	26	12
48 kHz	12	23	23	51	23
64 kHz	16	30	30	68	31
96 kHz	23	44	45	102	46
1 MHz	124	434	455	1054	479

$N*m$ users in a $B*m$ bandwidth. Besides, with an increased number of users, some insignificant interference contributions sum up to a significant level.

Finally, we can estimate that, for a $BER = 10^{-3}$ and $BW = 96$ kHz, the network is able to serve 10 simultaneous users. Considering average transmission duration of 1 second, the system will be able to handle around 864 000 transmissions per day, which corresponds for a 50 km radius to a density of 110 nodes per km^2: i.e., 3 times the USA population density.

V. Conclusion

In this paper, we have studied a new technology based on UNB transmission, considered for IoTs networks. This technology is used jointly with R-FDMA scheme, which, to the best of our knowledge, has not been studied yet in the literature in terms of interference and capacity. To evaluate the interference impact, we have considered the BER and the OP of the system in the R-FDMA case, where the users are randomly distributed. We have studied the influence of aggregate interference power for such networks. To this aim, we have presented a rectangular model, used to derive lower bound, upper bound, and approximated model of the system. We have shown the accuracy of the models. Then, thanks to their simplicity, we have theoretically evaluated the system performance (in term of BER and OP), and the capacity of the network in terms of possible number of active users. Thus, this study is a first step in the analysis of the promising UNB networks, can be furthered by considering the case where the received powers are different among the users, to take into account the cell geometry.

Acknowledgment

The authors would like to thank Christophe Fourtet (Sigfox) his helpful advices during this study.

References

[1] L. Mainetti, L. Patrono, and A. Vilei, “Evolution of wireless sensor networks towards the Internet of Things: A survey,” 19th International Conference on Software, Telecommunications and Computer Networks (SoftCOM), Split - Hvar - Dubrovnik, Croatia, 15-17 Sept. 2011, pp. 1-6.

[2] Ye Li, Dengyu Qiao, Zhao Xu, Da Xu, Fen Miao, and Yuwei Zhang, “Energy-Model-Based Optimal Communication Systems Design for Wireless Sensor Networks,” International Journal of Distributed Sensor Networks, vol.2012, 2012.

[3] Pei Huang, Li Xiao, S. Soltani, M. W Mutka, and Ning Xi, “The Evolution of MAC Protocols in Wireless Sensor Networks: A Survey,” Communications Surveys and Tutorials, IEEE, vol.15, no.1, First Quarter 2013, pp.101-120.

[4] A. Bachir, M. Dohler, T. Watteyne, and K.K Leung, “MAC Essentials for Wireless Sensor Networks,” Communications Surveys and Tutorials, IEEE, vol.12, no.2, Second Quarter 2010, pp. 222-248.

[5] H. K. Le, D. Henriksson, and T. Abdelzaher, “A Practical Multi-channel Media Access Control Protocol for Wireless Sensor Networks,” International Conference on Information Processing in Sensor Networks, IPSN’08, St. Louis, Missouri, USA, 22-24 April 2008.

[6] Y. Wu, J.A. Stankovic, T. He, and S. Lin, “Realistic and Efficient Multi-Channel Communications in Wireless Sensor Networks,” The 27th Conference on Computer Communications. IEEE, INFOCOM 2008, Phoenix, AZ, USA, 13-18 April 2008.

[7] Q. Yu, J. Chen, Y. Fan, X. Shen, and Y. Sun, “Multi-Channel Assignment in Wireless Sensor Networks: A Game Theoretic Approach,” Proceedings IEEE, INFOCOM 2010, San Diego, CA, USA, 14-19 March 2010.

[8] M. T. Do, C. Goursaud, and J. M. Gorce, “On the Benefits of Random FDMA Schemes in Ultra Narrow Band Networks,” to be presented in International Workshop on Wireless Networks: Communication, Cooperation and Competition, WNC3’14, Hammamet, Tunisia, 12-16 May 2014.

[9] M.Z. Win, P.C. Pinto, and L.A. Shepp, “A Mathematical Theory of Network Interference and Its Applications,” Proceedings of the IEEE, vol.97, no.2, Feb. 2009, pp. 205-230.

[10] M. Haenggi, and R. K. Ganti, “Interference in Large Wireless Networks,” Foundations and Trends in Networking, vol. 3, no. 2, 2008, pp. 127-248.

[11] M. Aljuaid, and H. Yanikomeroglu, “Investigating the Gaussian Convergence of the Distribution of the Aggregate Interference Power in Large Wireless Networks,” IEEE Transactions on Vehicular Technology, vol.59, no.9, Nov. 2010, pp. 4418-4424.

[12] H. Inaltekin, and S.V. Hanly, “On the rates of convergence of the wireless multi-access interference distribution to the normal distribution,” Proceedings of the 8th International Symposium on Modeling and Optimization in Mobile, Ad Hoc and Wireless Networks (WiOpt), May 31 2010-June 4 2010, pp. 453-458.

[13] H. Inaltekin, “Gaussian Approximation for the Wireless Multi-access Interference Distribution and Its Application”, Journal IEEE, 2012.

[14] M. Aljuaid, and H. Yanikomeroglu, “A Cumulant-Based Characterization of the Aggregate Interference Power in Wireless Networks,” Vehicular Technology Conference (VTC 2010-Spring), 16-19 May 2010, pp. 1-5.

[15] J. Riihijarvi, and P. Mahonen, “A model based approach for estimating aggregate interference in wireless networks,” International ICST Conference on Cognitive Radio Oriented Wireless Networks and Communications (CROWNCOM), 18-20 June 2012, pp. 180-184.

[16] www.sigfox.com/en/, May 2014.